

# Newton Method based Iterative Learning Control of the Upper Limb

I. L. Davies, C. T. Freeman, P. L. Lewin, E. Rogers and D. H. Owens

**Abstract**—A non-linear iterative learning control algorithm is used for the application of functional electrical stimulation to the human arm. The task is to track trajectories in the horizontal plane and stimulation is applied to the triceps muscle. A model of the system is first produced, and then the equations required to implement the control law are derived. Practical considerations are high-lighted and the issue of parameter selection is discussed. Experimental results are subsequently presented, and are used to confirm that the algorithm is capable of exhibiting robustness together with achieving a high level of performance when practically applied to a control problem.

## I. INTRODUCTION

Strokes affect between 174 and 216 people per 100,000 population in the UK each year, and half of all acute stroke patients starting rehabilitation will have a marked impairment of function in one arm [1]. Functional electrical stimulation (FES) can provide the experience of moving for the patient, which is necessary if sensory-motor function is to be regained. Recent studies have shown that when stimulation is associated with a voluntary attempt to move the limb, improvement is enhanced [2]. Open-loop methods for the control of FES (see, for example, [3]) have not provided the high level of performance necessary to fully promote this association. Closed-loop and model-based schemes, however, have overwhelmingly concentrated on the lower rather than the upper limb. Neural networks are one of the few approaches that have successfully been used to control FES applied to the arm, but these require extensive training and have unresolved stability issues due to their black-box structure [4].

An experimental test facility incorporating a five-link planar robotic arm and an overhead trajectory projection system (see [5] for details) has been developed in order to provide a controlled environment in which to apply electrical stimulation to stroke patients. The subject is seated with their arm strapped to the robot, and the task presented to them is to repeatedly track a number of reaching trajectories using a combination of voluntary control and surface FES applied to muscles in their impaired shoulder and arm. The electrical stimulation is mediated using iterative learning control (ILC), a technique that is applicable to systems operating in a cyclical mode. This is one of the few advanced control techniques which has previously been applied to stimulation

of the upper limb, although a high level of performance has not been achieved in practice [6].

In this paper a non-linear ILC algorithm is employed to control the FES applied to the triceps of an unimpaired subject who provides no voluntary effort. This not only tests the controller in the absence of voluntary action (which may be represented as a repeating disturbance acting on the system) in order to confirm the efficacy of the system prior to its use by stroke patients, but also establishes the performance that may be expected if it were used by hemiplegic patients unable to apply such effort. The algorithm is based on that developed in [7], in which the non-linear ILC problem is decomposed into a sequence of linear time-varying ILC problems each of which can be solved by applying any globally convergent ILC scheme. During each trial the robot supplies an assistive torque about the shoulder to allow full reaching tasks to be accomplished in a manner that is completely driven by the stimulation.

## II. WORKSTATION DESCRIPTION

The robotic workstation consists of a five-link planar robotic arm rigidly connected to an overhead projection system, and is shown in Figure 1. A subject is strapped to

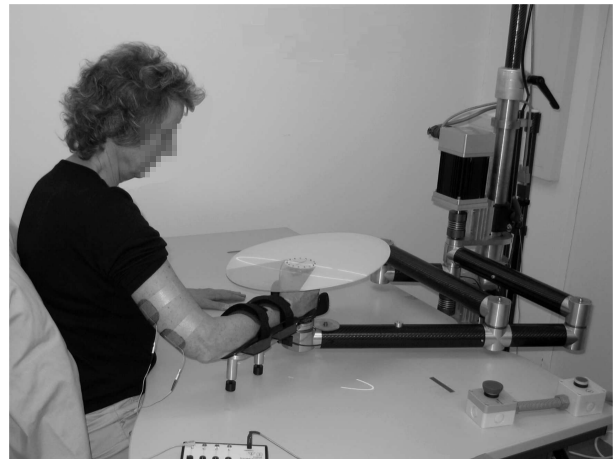


Fig. 1. Unimpaired subject using the robotic workstation.

the extreme link and a 6 axis force/torque sensor records the force they apply to the robotic end effector. The robotic arm is used to constrain the subject's arm, to impose forces on the end-effector that make the task feel 'natural' to the subject, and to apply assistance during the performance of tracking tasks. The stroke patient's task during the treatment will be to track a range of trajectories that are projected onto a target mounted above their hand. Further details

This work is supported by the Engineering and Physical Sciences Research Council (EPSRC). Grant no. EP/C51873X/1.

I. L. Davies, C. T. Freeman, P. L. Lewin and E. Rogers are with the School of Electronics and Computer Science, University of Southampton, Southampton, SO17 1BJ, UK. D. H. Owens is with the Department of Automatic Control and Systems Engineering, University of Sheffield, Mappin Street, Sheffield, S1 3JD, UK. cf@ecs.soton.ac.uk

regarding the design and functionality of the workstation and its peripheral systems are given in [5].

### III. HUMAN ARM MODEL

The description of the subject's arm consists of a model of the passive dynamical system to which the torque generating properties of the stimulated muscle is then added.

#### A. Passive System

Figure 2 shows the geometry of the constrained human arm model. The first link represents the upper arm, from the acromion to the elbow, with length  $l_u = (l_{u1} + l_{u2})$ . The second link represents the forearm, from the elbow to the thumb web, with length  $l_f = (l_{f1} + l_{f2})$ . The constraint means that the forearm must lie in the horizontal plane, and rotation is possible about the axis along the upper arm. The point,  $Q$ , denotes where the subject's hand grasps the robot, and components of the forces applied in the  $x_0$  and  $y_0$  directions are denoted by  $F_{x_0}$  and  $F_{y_0}$  respectively. Actuation is provided by the triceps, which has been modelled as supplying a torque,  $T_\beta \geq 0$ , acting about an axis orthogonal to both the upper arm and forearm. To satisfy the horizontal constraint

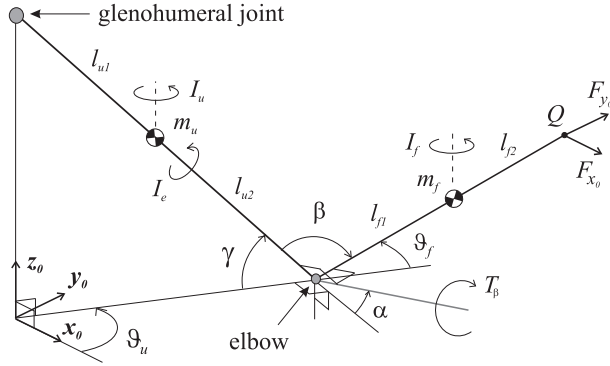


Fig. 2. Geometry of constrained human arm.

it is necessary to set

$$\alpha(\vartheta_f, \gamma) = \arccos\left(\frac{c_f s_\gamma}{\sqrt{1 - c_f^2 c_\gamma^2}}\right) \quad (1)$$

which corresponds to an elbow angle of

$$\beta(\vartheta_f, \gamma) = \arccos(-c_f c_\gamma) \quad (2)$$

Here  $c_f$  and  $c_\gamma$  denote  $\cos(\vartheta_f)$  and  $\cos(\gamma)$  respectively,  $c_u$  and  $c_{uf}$  will be used to denote  $\cos(\vartheta_u)$  and  $\cos(\vartheta_u + \vartheta_f)$ , and similarly for the case of  $\sin(\cdot)$ . The unitary axis about which  $T_\beta$  is applied is given by

$$\frac{1}{\sqrt{1 - c_f^2 c_\gamma^2}} \begin{bmatrix} -s_f s_\gamma \\ c_f s_\gamma \\ -s_f c_\gamma \end{bmatrix} \quad (3)$$

The dynamic model of the constrained arm can then be expressed in the form

$$\mathbf{B}(\mathbf{q})\ddot{\mathbf{q}} + \mathbf{C}(\mathbf{q}, \dot{\mathbf{q}})\dot{\mathbf{q}} + \mathbf{F}(\mathbf{q}, \dot{\mathbf{q}}) = \boldsymbol{\tau} - \mathbf{J}^T(\mathbf{q})\mathbf{h} \quad (4)$$

where  $\mathbf{q} = [\vartheta_u \ \vartheta_f]^T$ ,  $\boldsymbol{\tau} = [0 \ T_\beta \ \sigma(\vartheta_f, \gamma)]^T$ ,  $\mathbf{h} = [F_{x_0} \ F_{y_0}]^T$  and

$$\mathbf{B}(\mathbf{q}) = \begin{bmatrix} b_1 & b_2 \\ b_2 & b_3 \end{bmatrix}, \quad \mathbf{C}(\mathbf{q}, \dot{\mathbf{q}}) = \begin{bmatrix} -2c_1 \dot{\vartheta}_f - c_1 \dot{\vartheta}_f \\ c_1 \dot{\vartheta}_u \quad c_2 \dot{\vartheta}_f \end{bmatrix}, \quad (5)$$

$$\mathbf{J}^T(\mathbf{q}) = \begin{bmatrix} -l_u c_\gamma s_u - l_f s_{uf} & l_u c_\gamma c_u + l_f c_{uf} \\ -l_f s_{uf} & l_f c_{uf} \end{bmatrix}$$

with

$$b_1 = m_u(l_{u1} c_\gamma)^2 + I_u + m_f(l_{f1}^2 + (l_u c_\gamma)^2 + 2l_u c_\gamma l_{f1} c_f) + I_f$$

$$b_2 = m_f(l_{f1}^2 + l_u c_\gamma l_{f1} c_f) + I_f, \quad b_3 = m_f l_{f1}^2 + I_f + I_e \left(\frac{s_\gamma}{1 - c_f^2 c_\gamma^2}\right)^2 \quad (6)$$

$$c_1 = m_f l_u c_\gamma l_{f1} s_f, \quad c_2 = -2I_e \left(\frac{s_\gamma^2 c_f s_f}{(1 - c_f^2 c_\gamma^2)^3}\right)$$

and

$$\sigma(\vartheta_f, \gamma) = -\frac{s_f c_\gamma}{\sqrt{1 - c_f^2 c_\gamma^2}} \quad (7)$$

The form of the friction term considered is

$$\mathbf{F}(\mathbf{q}, \dot{\mathbf{q}}) = [F_1(\vartheta_u, \dot{\vartheta}_u) \ F_2(\vartheta_f, \dot{\vartheta}_f)]^T \quad (8)$$

in which  $F_1(\cdot)$  and  $F_2(\cdot)$  are piecewise linear functions. The  $\gamma$ -dependence of  $\alpha(\cdot)$ ,  $\beta(\cdot)$  and  $\sigma(\cdot)$  will now be dropped.

A form of impedance control (see [8]) is used to control the robotic arm, which results in the relationship

$$-\mathbf{h} = \mathbf{K}_{K_x} \tilde{\mathbf{x}} - \mathbf{K}_{B_x} \dot{\tilde{\mathbf{x}}} - \mathbf{K}_{M_x} \ddot{\tilde{\mathbf{x}}} \quad (9)$$

at  $Q$ , where  $\tilde{\mathbf{x}}$  is the reference position,  $\tilde{\mathbf{x}} = \hat{\mathbf{x}} - \mathbf{x}$ ,  $\mathbf{x} = \mathbf{k}(\mathbf{q})$ ,  $\dot{\mathbf{x}} = \mathbf{J}(\mathbf{q})\dot{\mathbf{q}}$  and  $\ddot{\mathbf{x}} = \mathbf{J}(\mathbf{q})\ddot{\mathbf{q}} + \dot{\mathbf{J}}(\mathbf{q}, \dot{\mathbf{q}})\dot{\mathbf{q}}$ . Here  $\mathbf{x} = \mathbf{k}(\mathbf{q})$  is the direct kinematics equation for the human arm system. When the robot is moved freely by the subject in the absence of assistance, the gain matrices are set as  $\mathbf{K}_{K_x} = \mathbf{0}$ ,  $\mathbf{K}_{B_x} = K_{B_x} \mathbf{I}$  and  $\mathbf{K}_{M_x} = K_{M_x} \mathbf{I}$ . The values of  $K_{B_x}$  and  $K_{M_x}$  assume positive values and are tuned to create a 'natural' feel. When the robot is required to move the subject's arm along predefined trajectories, it is necessary to set  $\mathbf{K}_{K_x} = K_{K_x} \mathbf{I}$  with  $K_{K_x} > 0$ . The three gains are then tuned to produce the required tracking performance. The form of the gain matrices for the case where the robot applies assistance during tracking tasks, is described in Section IV. Further details of the robotic controller are given in [5].

#### B. Muscle Model

A model of the torque,  $T_\beta$ , generated by electrically stimulated muscle acting about a single joint is given by

$$T_\beta(\beta, \dot{\beta}, u, t) = h_\beta(u, t) \times F_a(\beta, \dot{\beta}) + F_p(\beta, \dot{\beta}) \quad (10)$$

where  $u$  denotes the stimulation pulsewidth applied, and  $\beta$  is the joint angle (see [9] for details). A Hammerstein structure incorporating a static non-linearity,  $h_{IRC}(u)$ , representing the isometric recruitment curve, cascaded with linear activation dynamics,  $h_{LAD}(t)$ , produces the first term,  $h_\beta(u, t)$ . The activation dynamics can be modelled as a critically damped second order system [10]. The term  $F_a(\beta, \dot{\beta})$  describes the multiplicative effect of the joint angle and joint angular velocity on the active torque developed by the muscle. The term  $F_p(\beta, \dot{\beta})$  accounts for the passive properties of the joint. Since  $\gamma$  is invariant, (2) means it is accounted for when using the frictional form of (8). A full description of the procedures used to establish the parameters appearing in the model, and also identification results similar to those of the subject whose results appear in Section VII, is given in [11].

#### IV. ROBOTIC ASSISTANCE

The trajectories used consist of constant velocity, elliptical reaching tasks for the subject's dominant arm. Ellipses have been chosen since they approximate functional reaching movements similar to those required to perform every-day tasks, but, using a suitable velocity, limit the level of higher order joint kinematics required to track them and thus can be used to provide a smooth movement for the subject to follow. Tracking of these trajectories is, however, not achievable using only stimulation applied to the triceps. The robot will therefore be used to provide a torque acting about the subject's shoulder in order to track the reference in a manner which is entirely governed by the angle of the forearm. The triceps muscle will meanwhile provide the sole actuating torque about the elbow, and the robotic arm will use the control scheme given by (9) to make the dynamics about this axis feel 'natural' to the subject. This then makes the task feasible without diminishing the role played by the triceps. To find the necessary robotic assistance, (9) and (4) are combined to give

$$\mathbf{B}(\mathbf{q})\ddot{\mathbf{q}} + \mathbf{C}(\mathbf{q}, \dot{\mathbf{q}})\dot{\mathbf{q}} + \mathbf{F}(\mathbf{q}, \dot{\mathbf{q}}) = \mathbf{J}^T(\mathbf{q}) \left( \mathbf{K}_{K_x} \tilde{\mathbf{x}} - \mathbf{K}_{B_x} \dot{\mathbf{x}} - \mathbf{K}_{M_x} \ddot{\mathbf{x}} \right) + \boldsymbol{\tau} \quad (11)$$

To separate the dynamics of the end-effector in the directions corresponding to the human arm joint angles, it is then necessary to set

$$\mathbf{K}_{K_x} \tilde{\mathbf{x}} - \mathbf{K}_{B_x} \dot{\mathbf{x}} - \mathbf{K}_{M_x} \ddot{\mathbf{x}} = \mathbf{J}^{-T}(\mathbf{q}) \left( \mathbf{K}_{K_q} \tilde{\mathbf{q}} - \mathbf{K}_{B_q} \dot{\mathbf{q}} - \mathbf{K}_{M_q} \ddot{\mathbf{q}} \right) \quad (12)$$

where  $\tilde{\mathbf{q}} = \hat{\mathbf{q}} - \mathbf{q}$  and  $\hat{\mathbf{q}} = \mathbf{k}^{-1}(\hat{\mathbf{x}})$ . It is then required that

$$\begin{aligned} \mathbf{K}_{K_q} &= \text{diag}\{K_{K_1}, 0\}, \quad \mathbf{K}_{B_q} = \text{diag}\{K_{B_1}, K_{B_2}\} \\ \mathbf{K}_{M_q} &= \text{diag}\{K_{M_1}, K_{M_2}\} \end{aligned} \quad (13)$$

and  $\hat{\mathbf{q}} = [\hat{\vartheta}_u \ \hat{\vartheta}_f]^T$  where  $K_{K_1}, K_{B_1}, K_{B_2}, K_{M_1}, K_{M_2} \geq 0$ . This allows a choice of arbitrary second order dynamics to be imposed about the shoulder and the damping and inertia about the elbow to be prescribed. This produces the expression

$$\begin{bmatrix} K_{K_1} \hat{\vartheta}_u - K_{B_1} \dot{\vartheta}_u - K_{M_1} \ddot{\vartheta}_u \\ -K_{B_2} \hat{\vartheta}_f - K_{M_2} \ddot{\vartheta}_f \end{bmatrix} + \boldsymbol{\tau} \quad (14)$$

for the right-hand side of (11), and provides the necessary dynamic relationship for both components of the torque. To arrive at the required values of  $\hat{\vartheta}_u$  and  $\hat{\vartheta}_f$ , components of (12) are compared to give

$$\mathbf{K}_{K_x} (\hat{\mathbf{x}} - \mathbf{x}) = \mathbf{J}^{-T}(\mathbf{q}) \begin{bmatrix} K_{K_1} (\hat{\vartheta}_u - \vartheta_u) \\ 0 \end{bmatrix} = \frac{K_{K_1} (\hat{\vartheta}_u - \vartheta_u)}{l_u c \gamma s_f} \begin{bmatrix} c_{uf} \\ s_{uf} \end{bmatrix}$$

This leads to a solution

$$\mathbf{K}_{K_x} = \frac{K_{K_1} (\hat{\vartheta}_u - \vartheta_u)}{|\hat{\mathbf{x}} - \mathbf{x}| l_u c \gamma s_f} \mathbf{I}, \quad \hat{\mathbf{x}} = \mathbf{x} + |\hat{\mathbf{x}} - \mathbf{x}| \begin{bmatrix} c_{uf} \\ s_{uf} \end{bmatrix} \quad (15)$$

so that  $\hat{\mathbf{x}}$  is a point lying on a line extending along the forearm and passing through  $\mathbf{x}$ . To achieve the tracking task it must therefore be set equal to the point of intersection with the trajectory. This is shown in Figure 3, in which

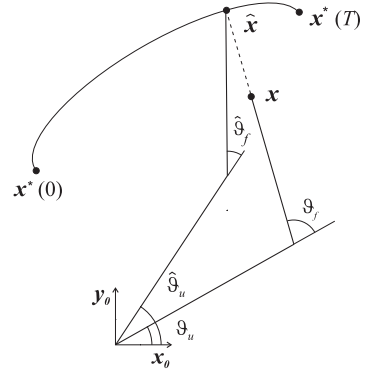


Fig. 3. Trajectory Geometry.

$\mathbf{x}^*(t) = \mathbf{k}(\mathbf{q}^*(t))$  with  $\mathbf{q}^*(t)$  defined in (17). The remaining robotic controller matrices may be chosen to satisfy

$$\begin{cases} \mathbf{K}_{B_x} = \mathbf{J}^{-T}(\mathbf{q}) \mathbf{K}_{B_q} \mathbf{J}^{-1}(\mathbf{q}) \\ \mathbf{K}_{M_x} (\mathbf{J}(\mathbf{q}) \ddot{\mathbf{q}} + \dot{\mathbf{J}}(\mathbf{q}, \dot{\mathbf{q}}) \dot{\mathbf{q}}) = \mathbf{J}^{-T}(\mathbf{q}) \mathbf{K}_{M_q} \end{cases} \quad (16)$$

with the gains given by (13). If the trajectory is defined as

$$\mathbf{q}^*(t) = [\vartheta_u^*(t) \ \vartheta_f^*(t)]^T, \quad t \in [0 \ T] \quad (17)$$

then eliminating  $t$  from the components provides the relationship  $\vartheta_u = \Psi(\vartheta_f)$  and for this to be a one-one continuous function, both  $\vartheta_u^*(t)$  and  $\vartheta_f^*(t)$  must be monotone. The reference point is then defined formally as

$$\hat{\mathbf{x}} = \boldsymbol{\Omega}(\mathbf{x}, \Psi(\cdot)) : \mathbf{k} \left( \begin{bmatrix} \Psi(\hat{\vartheta}_f) \\ \hat{\vartheta}_f \end{bmatrix} \right) \Big| \mathbf{k} \left( \begin{bmatrix} \Psi(\hat{\vartheta}_f) \\ \hat{\vartheta}_f \end{bmatrix} \right) = \mathbf{x} + \lambda \begin{bmatrix} c_{uf} \\ s_{uf} \end{bmatrix}$$

where  $\lambda$  is a scalar. The complete control system is shown in Figure 4. The gain (15) can then be written explicitly as

$$\mathbf{K}_{K_x}(\mathbf{x}, \Psi(\cdot)) = \frac{K_{K_1} (\Psi(\hat{\vartheta}_f) - \vartheta_u)}{\lambda l_u c \gamma s_f} \mathbf{I} \quad (18)$$

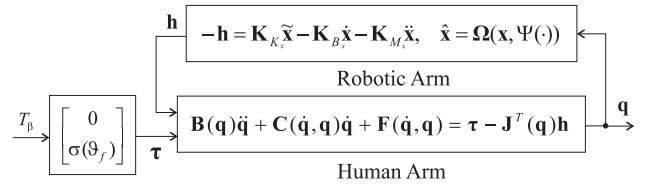


Fig. 4. Human arm system with robotic assistance.

It is now assumed that the robotic assistance system provides accurate tracking of  $\hat{\vartheta}_u$  by  $\vartheta_u$ , so that  $\vartheta_u = \Psi(\vartheta_f)$ , then  $\dot{\vartheta}_u = \dot{\vartheta}_f \Psi'(\vartheta_f)$  and  $\ddot{\vartheta}_u = \ddot{\vartheta}_f \Psi'(\vartheta_f) + \dot{\vartheta}_f^2 \Psi''(\vartheta_f)$ . Moreover the relationship  $c_1, c_2 \ll b_2, b_3$  holds for the robotic arm, and furthermore  $I_e \approx 0.005 \text{ Kg m}^2$  (see [11] for examples of identified muscle model parameters), and the trajectories are chosen so that the derivatives of  $\Psi(\cdot)$  are small. Therefore the bottom row of (11), with the expressions given by (9) and (12), and the control gains (13), produces

$$T_\beta \approx \frac{1}{\sigma(\vartheta_f)} (K_{B_2} \dot{\vartheta}_f + (b_3 + K_{M_2}) \ddot{\vartheta}_f + F_2(\vartheta_f, \dot{\vartheta}_f)) \quad (19)$$

which is shown schematically in Figure 5. In practice the existence of a torque that will allow  $\vartheta_f^*(t)$  to be tracked

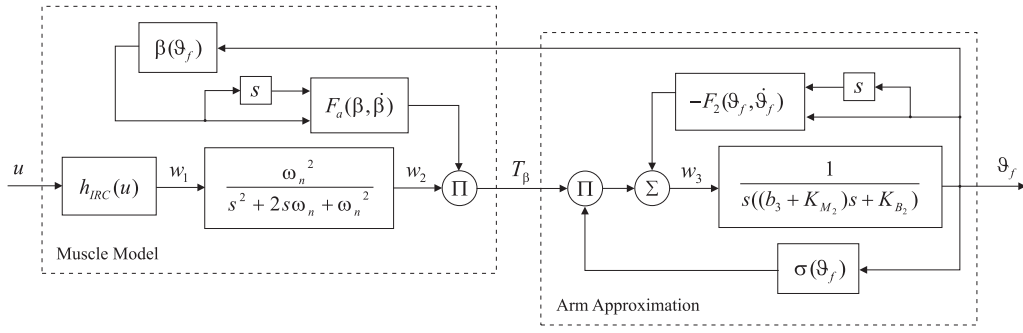


Fig. 5. Continuous-time model of stimulated human arm showing feedback loops.

perfectly is ensured by selecting trajectories that comprise half ellipse segments whose start and end points can be reached by a smooth extension about the elbow. The gains,  $K_{B_2}$  and  $K_{M_2}$ , were selected as  $8 \text{ Nm/rads}^{-1}$  and  $0.29 \text{ Nm/rads}^{-2}$  respectively in order to mimic a realistic activity.

## V. IDENTIFIED PARAMETERS

The parameters appearing in the arm model (4) were identified using tests described in [11]. In particular FES was applied to the subject's triceps using a ramp signal, and  $h_{IRC}(u)$  and  $h_{LAD}(t)$  were found using deconvolution and a non-linear optimisation procedure. Suitably rich stimulation sequences and kinematic trajectories were then applied to the arm and an LMS optimisation was used to yield the remaining model parameters. The values produced were  $l_u = 0.38\text{m}$ ,  $l_f = 0.39\text{m}$ ,  $\gamma = 0.7928\text{rad}$ ,  $\omega_n = 2.6704\text{rads}^{-1}$ ,  $b_3 = 0.27\text{Kgm}^2$ , along with the function  $h_{IRC}(u) = 0.1695 \frac{\exp(-1.1891u)-1}{\exp(-1.1891u)+0.2723}$ , and the forms of  $F_2(\vartheta_f, \dot{\vartheta}_f)$  and  $F_a(\beta, \dot{\beta})$  that are shown in Figures 6 and 7 respectively. Figure 8 shows the shape of the reference used

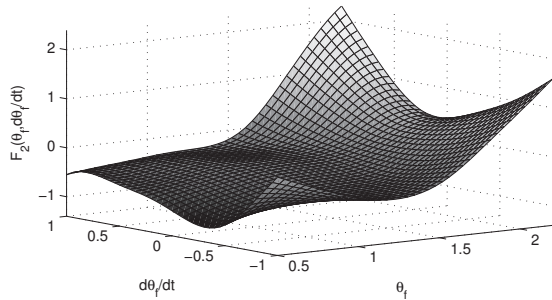


Fig. 6. Combined viscous and elastic friction function  $F_2(\vartheta_f, \dot{\vartheta}_f)$ .

to produce the results in this paper. It is set at an angle of  $20^\circ$  from the y axis and extends the subject's arm from 55% to 95% of their maximum reach. The trajectory consists of a 5 second waiting period and either a 2.5, 5 or 7.5 second movement along the reference at a constant speed, these respectively being termed fast, medium and slow trajectories (Figure 11 shows  $\vartheta_f^*(t)$  corresponding to the medium trajectory). Before each trial began, the subject's arm was moved to the initial position by the robot and then released when the trajectory started. The subject was not shown the trajectory

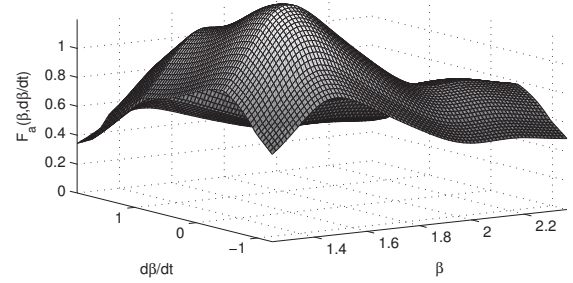


Fig. 7. Active muscle function  $F_a(\beta, \dot{\beta})$ .

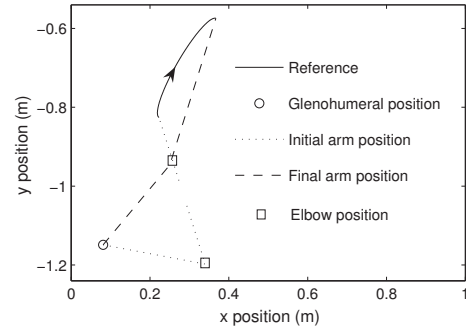


Fig. 8. Reference trajectory and position of subject tested.

before or during the test and electromyographic data were inspected to ensure no voluntary effort was exerted by them.

## VI. SYSTEM DESCRIPTION

To produce a discrete-time system representation, let the linear activation dynamics be represented by the state-space system in standard form  $[\Phi_m, \Gamma_m, \mathbf{H}_m]$ . The relationship between  $w_1$  and  $w_2$  shown in Figure 5 is then given by

$$\begin{aligned} \mathbf{x}_m(t+1) &= \Phi_m \mathbf{x}_m(t) + \Gamma_m w_1(t) & \mathbf{x}_m(0) &= \mathbf{x}_{m0} \\ w_2(t) &= \mathbf{H}_m \mathbf{x}_m(t) \end{aligned} \quad (20)$$

and similarly the arm dynamics be represented by the state-space system  $[\Phi_p, \Gamma_p, \mathbf{H}_p]$  so that the relationship between  $w_3$ ,  $\vartheta_f$  and  $\dot{\vartheta}_f$  is given by

$$\begin{aligned} \mathbf{x}_p(t+1) &= \Phi_p \mathbf{x}_p(t) + \Gamma_p w_3(t) & \mathbf{x}_p(0) &= \mathbf{x}_{p0} \\ \begin{bmatrix} \vartheta_f(t) \\ \dot{\vartheta}_f(t) \end{bmatrix} &= \begin{bmatrix} \mathbf{H}_{p1} \\ \mathbf{H}_{p2} \end{bmatrix} \mathbf{x}_p(t) = \mathbf{H}_p \mathbf{x}_p(t) \end{aligned} \quad (21)$$

In this case the system is given on trial  $k$  by

$$\begin{aligned} \mathbf{x}_k(t+1) &= \mathbf{\Phi}\mathbf{x}_k(t) + \mathbf{\Gamma} \begin{bmatrix} d(\mathbf{x}_k(t)) \\ h_{IRC}(u_k(t)) \end{bmatrix} = \mathbf{f}(\mathbf{x}_k(t), u_k(t)) \\ \vartheta_{f,k}(t) &= \bar{\mathbf{H}}_{p_1}\mathbf{x}_k(t) = \mathbf{h}(\mathbf{x}_k(t)) \quad \mathbf{x}_k(0) = \mathbf{x}_0 \quad t \in [0, N] \end{aligned} \quad (22)$$

where  $\mathbf{x}(t) = [\mathbf{x}_p(t) \ \mathbf{x}_m(t)]^T$ ,  $\mathbf{x}_0 = [\mathbf{x}_{p0} \ \mathbf{x}_{m0}]^T$ ,  $\mathbf{\Phi} = \text{diag}\{\mathbf{\Phi}_p, \mathbf{\Phi}_m\}$ ,  $\mathbf{\Gamma} = \text{diag}\{\mathbf{\Gamma}_p, \mathbf{\Gamma}_m\}$ ,  $\bar{\mathbf{H}}_m = [\mathbf{0} \ \mathbf{H}_m]$ ,  $\bar{\mathbf{H}}_{p_1} = [\mathbf{H}_{p_1} \ \mathbf{0}]$  and  $\bar{\mathbf{H}}_{p_2} = [\mathbf{H}_{p_2} \ \mathbf{0}]$ . The integer  $N$  is equal to  $\frac{T}{T_s} + 1$ , where  $T_s$  is the sample time, and

$$\begin{aligned} d(\mathbf{x}_k) &= \bar{\mathbf{H}}_m\mathbf{x}_k F_a (\beta (\bar{\mathbf{H}}_{p_1}\mathbf{x}_k), \bar{\mathbf{H}}_{p_2}\mathbf{x}_k\beta' (\bar{\mathbf{H}}_{p_1}\mathbf{x}_k)) \sigma (\bar{\mathbf{H}}_{p_1}\mathbf{x}_k) \\ &\quad - F_2 (\bar{\mathbf{H}}_{p_1}\mathbf{x}_k, \bar{\mathbf{H}}_{p_2}\mathbf{x}_k) \end{aligned} \quad (23)$$

in which the explicit time dependence of  $\mathbf{x}_k$  has been omitted. To replace (22) with a set of algebraic equations in  $\mathbb{R}^N$ , define the shifted input and output vectors as

$$\begin{aligned} \mathbf{u}_k &= [u_k(0), u_k(1), \dots, u_k(N-1)]^T \\ \vartheta_{f,k} &= [\vartheta_{f,k}(1), \vartheta_{f,k}(2), \dots, \vartheta_{f,k}(N)]^T \end{aligned} \quad (24)$$

and the relationship between the input and output time-series can be expressed by the following algebraic functions

$$\begin{aligned} \vartheta_{f,k}(1) &= \mathbf{h}(\mathbf{x}_k(1)) = \mathbf{h}(\mathbf{f}(\mathbf{x}_k(0), u_k(0))) = g_1(\mathbf{x}_k(0), u_k(0)) \\ \vartheta_{f,k}(2) &= \mathbf{h}(\mathbf{x}_k(2)) = \mathbf{h}(\mathbf{f}(\mathbf{x}_k(1), u_k(1))) = g_2(\mathbf{x}_k(0), u_k(0), u_k(1)) \\ &\vdots \\ \vartheta_{f,k}(N) &= \mathbf{h}(\mathbf{x}_k(N)) = \mathbf{h}(\mathbf{f}(\mathbf{x}_k(N-1), u_k(N-1))) \\ &= g_N(\mathbf{x}_k(0), u_k(0), u_k(1), \dots, u_k(N-1)) \end{aligned} \quad (25)$$

so that the system (22) can be represented as

$$\vartheta_{f,k} = \mathbf{g}(\mathbf{u}_k), \quad \mathbf{g}(\cdot) = [g_1(\cdot), g_2(\cdot), \dots, g_N(\cdot)]^T \quad (26)$$

The ILC task of finding the input which drives the dynamic system (22) to track the desired output, becomes finding the solution that satisfies the non-linear function (26) with  $\vartheta_{f,k}$  substituted by  $\vartheta_f^* = [\vartheta_f^*(1), \vartheta_f^*(2), \dots, \vartheta_f^*(N)]^T$ . The Newton method is selected to solve this non-linear equation, and is given in ILC notation as

$$\mathbf{u}_{k+1} = \mathbf{u}_k + \alpha_{k+1} \mathbf{g}'(\mathbf{u}_k)^{-1} \mathbf{e}_k \quad (27)$$

where the scalar  $\alpha_{k+1} \geq 0$  is a relaxation parameter, and  $\mathbf{e}_k = \vartheta_f^* - \vartheta_{f,k}$ . The derivative  $\mathbf{g}'(\mathbf{u}_k)$  is equivalent to the linearisation of (22), on the  $k^{\text{th}}$  iteration at  $(\mathbf{u}_k, \mathbf{x}_k)$  which can be represented by the time-varying system

$$\tilde{\vartheta}_f = \mathbf{g}'(\mathbf{u}_k) \tilde{\mathbf{u}} \quad (28)$$

which is given by

$$\begin{aligned} \tilde{\mathbf{x}}(t+1) &= \mathbf{A}(t)\tilde{\mathbf{x}}(t) + \mathbf{B}(t)\tilde{\mathbf{u}}(t) \\ \tilde{\vartheta}_f(t) &= \mathbf{C}(t)\tilde{\mathbf{x}}(t) \end{aligned} \quad (29)$$

with

$$\begin{aligned} \mathbf{A}(t) &= \left( \frac{\partial \mathbf{f}}{\partial \mathbf{x}} \right)_{\mathbf{u}_k(t), \mathbf{x}_k(t)} = \mathbf{\Phi} + \mathbf{\Gamma} \begin{bmatrix} \mathbf{p}(t) \\ \mathbf{0} \end{bmatrix} \\ \mathbf{B}(t) &= \left( \frac{\partial \mathbf{f}}{\partial \mathbf{u}} \right)_{\mathbf{u}_k(t), \mathbf{x}_k(t)} = \mathbf{\Gamma} \begin{bmatrix} 0 \\ h'_{IRC}(u_k(t)) \end{bmatrix} \\ \mathbf{C}(t) &= \left( \frac{\partial \mathbf{h}}{\partial \mathbf{x}} \right)_{\mathbf{u}_k(t), \mathbf{x}_k(t)} = \bar{\mathbf{H}}_{p_1} \end{aligned} \quad (30)$$

where  $\tilde{\mathbf{x}} = \mathbf{x}_{k+1} - \mathbf{x}_k$ ,  $\tilde{\mathbf{u}} = \mathbf{u}_{k+1} - \mathbf{u}_k$ ,  $\tilde{\vartheta}_f = \vartheta_{f,k+1} - \vartheta_{f,k}$ ,  $\tilde{\mathbf{x}}(0) = \mathbf{x}_{k+1}(0) - \mathbf{x}_k(0) = \mathbf{0}$  and

$$\begin{aligned} \mathbf{p}(t) &= \bar{\mathbf{H}}_m F_a \sigma + \bar{\mathbf{H}}_m \mathbf{x} \bar{\mathbf{H}}_{p_1} \beta' F_a' \sigma + \bar{\mathbf{H}}_m \mathbf{x} F_a \bar{\mathbf{H}}_{p_1} \sigma' - \bar{\mathbf{H}}_{p_1} F_2' \\ &\quad + \bar{\mathbf{H}}_m \mathbf{x} (\bar{\mathbf{H}}_{p_2} \beta' + \bar{\mathbf{H}}_{p_2} \mathbf{x} \bar{\mathbf{H}}_{p_1} \beta'') F_a' \sigma - \bar{\mathbf{H}}_{p_2} F_2^* \end{aligned} \quad (31)$$

where  $*$  denotes differentiation with respect to the second variable, and the functional dependence has been omitted. If the system (28) can be made to track  $\mathbf{e}_k$ , then the corresponding input is  $\tilde{\mathbf{u}} = \mathbf{g}'(\mathbf{u}_k)^{-1} \mathbf{e}_k$  which can then be used in the update (27). In this paper the Norm Optimal ILC (NOILC) method has been used to do this (see [12] for details), thereby obviating the problem of calculating the inverse of  $\mathbf{g}'(\mathbf{u}_k)$  directly. Using this method, the input to (28) on the  $(m+1)^{\text{th}}$  trial is chosen to minimise

$$\begin{aligned} J_{m+1} &= \sum_{t=1}^N [e_k(t) - \tilde{\vartheta}_{f,m+1}(t)]^T Q [e_k(t) - \tilde{\vartheta}_{f,m+1}(t)] \\ &\quad + \sum_{t=0}^{N-1} [\tilde{u}_{m+1}(t) - \tilde{u}_m(t)]^T R [\tilde{u}_{m+1}(t) - \tilde{u}_m(t)] \end{aligned} \quad (32)$$

In practice only a limited number,  $M$ , of iterations of NOILC have been performed since using a great number typically leads to  $\tilde{\mathbf{u}}$  containing large values, which, when used in (27), will saturate the muscle model (since the pulsewidth of the stimulation applied was limited to  $300\mu\text{s}$ ) and lead to greater discrepancy between the system and the linear model approximation at these points.

## VII. RESULTS

The algorithm was tested on a 60 year old subject (and so age-matched with future stroke patients). The NOILC parameters were selected as  $M = 30$ ,  $Q = 50000$  and  $R = 1$  in order to produce an update which tracks the error well but does not produce an excessively large input. Figure 9 shows error results for the medium trajectory over 20 trials using various values of  $\alpha$ . The value of  $\|e_k\|_2$  is plotted against  $k$  and it can be seen that the fastest convergence occurs using  $\alpha = 0.3$ , and the lowest error is less than 3mm. Figure 10 shows error results for the fast trajectory, in this

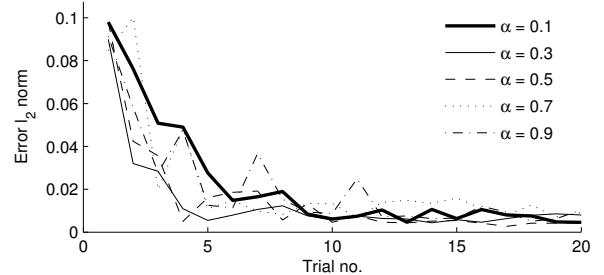


Fig. 9. Medium trajectory error results using various  $\alpha$ .

case  $\alpha = 0.3$  again yields the fastest convergence, and the lowest error is again less than 3mm. Figure 11 a) shows tracking results using the fast trajectory with  $\alpha = 0.3$ . The reference is seen to be closely followed by the fifth iteration, and the corresponding stimulation pulsewidth,  $u_k$ , shown in Figure 11 b), is not excessive. The parameter  $\alpha$  can be used

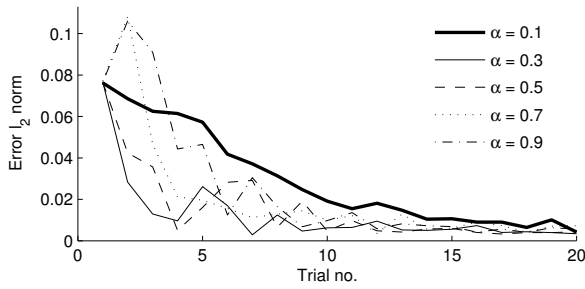


Fig. 10. Fast trajectory error results using various  $\alpha$ .

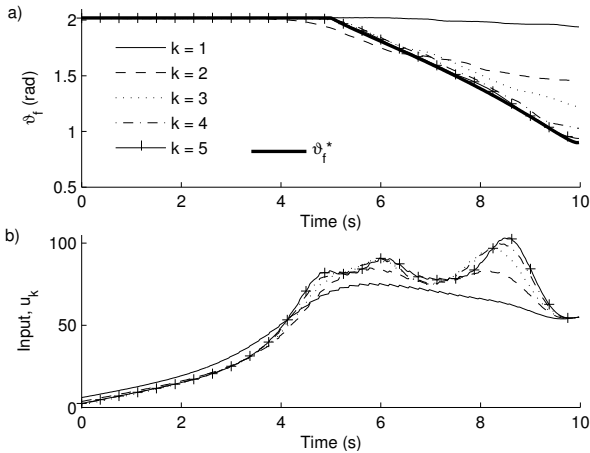


Fig. 11. a) Tracking and b) input signals using medium trajectory with  $\alpha = 0.3$ .

to ensure monotonic convergence in the presence of severe nonlinearity, and has accordingly been chosen by optimising

$$\min J_{k+1}(\alpha_{k+1}) = \|\mathbf{e}_{k+1}\|^2 = \|\boldsymbol{\vartheta}_f^* - \mathbf{g}(\mathbf{u}_k + \alpha_{k+1}\mathbf{z}_{k+1})\|^2 \quad (33)$$

where  $\mathbf{z}_{k+1}$  is the approximation to  $\mathbf{g}'(\mathbf{u}_k)^{-1}\mathbf{e}_k$  produced by the NOILC algorithm. The value of  $\alpha_{k+1}$  was chosen using a search method with a resolution of 0.05, and Figure 12 a) shows error results using this optimisation procedure for all three trajectories. It can be seen that faster convergence has been achieved in each case than when using a fixed value of  $\alpha$ . The associated values of  $\alpha_{k+1}$  are shown in Figure 12 b).

### VIII. CONCLUSION

A Newton based non-linear ILC method has been used to apply stimulation to the upper arm of unimpaired subjects in order to establish the feasibility of its use with hemiplegic and stroke patients. The equations governing the system have been derived along with those required for the algorithm implementation. The NOILC algorithm has been used to provide the required input update, together with an optimal gain. Results using trajectories of varying speeds have shown that tracking with a mean of less than 3mm is possible in each case.

To increase the performance of the Newton-based ILC algorithm, future research will concentrate on its application to the system comprising the stimulated arm system in

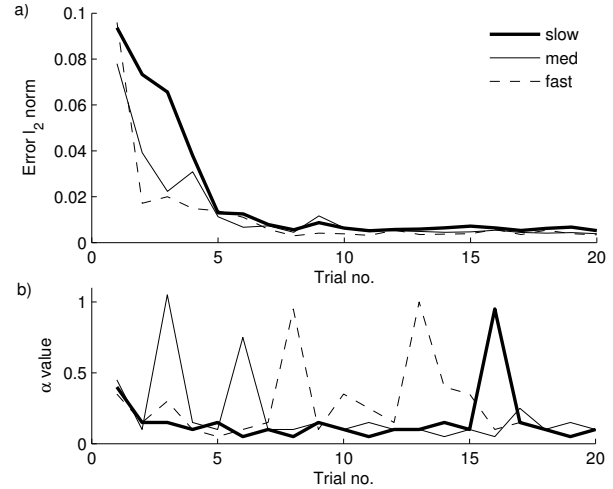


Fig. 12. a) error results and b)  $\alpha$  values for fast, medium and slow trajectory using optimal  $\alpha$ .

conjunction with various forms of feedback controller. The ability of the algorithm to adapt to time-varying effects such as muscle fatigue will also be examined.

### REFERENCES

- [1] J. Mant, D. Wade, and S. Winner, "Health care needs assessment: stroke," in *Health care needs assessment: the epidemiologically based needs assessment reviews*, A. Stevens, J. Raftery, J. Mant, and S. Simpson, Eds. Oxford: Radcliffe Medical Press, 2004.
- [2] J. H. Burridge and M. Ladouceur, "Clinical and therapeutic applications of neuromuscular stimulation: A review of current use and speculation into future developments," *Neuromodulation*, vol. 4, no. 4, pp. 147–154, 2001.
- [3] R. Davoodi and B. J. Andrews, "Fuzzy logic control of FES rowing exercise in paraplegia," *IEEE Transactions on Biomedical Engineering*, vol. 51, no. 3, pp. 541–543, 2004.
- [4] N. Lan, H. Q. Feng, and P. E. Crago, "Neural network generation of muscle stimulation patterns for control of arm movements," *IEEE Transactions on Rehabilitation Engineering*, vol. 2, no. 4, pp. 213–224, December 1994.
- [5] C. T. Freeman, A. M. Hughes, J. H. Burridge, P. H. Chappell, P. L. Lewin, and E. Rogers, "An experimental facility for the application of iterative learning control as an intervention aid to stroke rehabilitation," *Measurement + Control: The Journal of the Institute of Measurement and Control*, vol. 40, no. 1, pp. 20–23, February 2007.
- [6] H. Dou, K. K. Tan, T. H. Lee, and Z. Zhou, "Iterative learning control of human limbs via functional electrical stimulation," *Control Engineering Practice*, vol. 7, pp. 315–325, 1999.
- [7] T. Lin, D. H. Owens, and J. J. Hätönen, "Newton method based iterative learning control for discrete non-linear systems," *International Journal of Control*, vol. 79, no. 10, pp. 1263–1276, 2006.
- [8] J. E. Colgate and N. Hogan, "Robust control of dynamically interacting systems," *International Journal of Control*, vol. 48, no. 1, pp. 65–88, 1988.
- [9] G. Shue, P. E. Crago, and H. J. Chizeck, "Muscle-joint models incorporating activation dynamics, moment-angle, and moment-velocity properties," *IEEE Transactions on Biomedical Engineering*, vol. 42, no. 2, pp. 213–223, February 1995.
- [10] R. Baratta and M. Solomonow, "The dynamic response model of nine different skeletal muscles," *IEEE Transactions on Biomedical Engineering*, vol. 37, no. 3, pp. 243–251, March 1990.
- [11] C. T. Freeman, A. M. Hughes, J. H. Burridge, P. H. Chappell, P. L. Lewin, and E. Rogers, "A model of the upper extremity using surface FES for stroke rehabilitation," *Submitted to Journal of Biomechanical Engineering*, 2008.
- [12] N. Amann, D. H. Owens, and E. Rogers, "Iterative learning control using optimal feedback and feedforward actions," *International Journal of Control*, vol. 65, no. 2, pp. 277–293, 1996.